Aalborg Universitet

Application of short-time Fourier transform for harmonic-based protection of meshed VSC-MTDC grids

Mani Ashouri[1] ✉, Filipe F.D. Silva[1], Claus L. Bak[1]

[1]*Aalborg University, Department of Energy Technology, Aalborg, Denmark*
✉ *E-mail: maa@et.aau.dk*

Abstract: This work studies the application of short-time Fourier transform (STFT) to extract current harmonics of various fault types to design a protection method for meshed multi-terminal voltage source converter-high-voltage direct current (VSC-HVDC-MTDC) grids. The frequency spectrum of fault current harmonics is used to detect internal and external faults, the faulty pole and fault type. The method does not need the implementation of series inductance on the sides of the DC lines and it is also effective for lines combining overhead lines and cables. The window function and hop size play the primary role in STFT, which are investigated in a sensitivity analysis. A modified version of CIGRE meshed DC grid system is simulated in PSCAD in order to show the robustness of the method, and further signal processing analysis is done in MATLAB. The results show the accurate detection and discrimination between faulty sections using the proposed harmonic-based method and how important the STFT parameters are in order to have a robust protection algorithm.

1 Introduction

Voltage source converter-based high-voltage DC transmission (VSC-HVDC) has a key role in future power transmission. It has many advantages over line commutated converter (LCC–HVDC) systems as better power flow control or the reversal of power without changing voltage polarities. Despite the benefits of VSC-HVDC, there are difficulties in the deployment of these systems, particularly in protection and control, when the future multi-terminal (VSC-MTDC) topologies are established. Among different multi-terminal topologies for VSC-HVDC grids, meshed topology has more complex power flow, protection and control challenges, which needs further studies and more robust methods to be developed.

The protection system for VSC-MTDC grids must be extremely fast, selective and reliable [1]. The protection process consists of fault detection, commanding the breakers and tripping. With the aid of future DC breakers, selective protection will be feasible, which is essential for VSC-MTDC grids.The latest proposed protection methods for VSC-MTDC grids are mostly based on travelling waves [2], frequency [3], voltage transient [4] and artificial intelligence [5].

Fault current and voltage harmonics also have useful information for defining protection algorithms for different HVDC topologies. Zheng *et al.* [6] presented a transient harmonic current protection scheme for LCC–HVDC transmission lines, using the complex form of discrete Fourier transform (DFT) to extract 12th, 24th and 36th harmonic orders of fault transients. The method is able to discriminate between internal and external faults in point to point topologies. A harmonic based protection method using the same complex DFT method and the first carrier frequency harmonic current is presented in [7], for VSC–HVDC systems. The method is also capable to discriminate between internal and external faults. However, no information about the ability to detect the faulty pole and type of fault is given in the results. Other than that, this paper only concentrated on different fault types of the AC part and had no investigation on DC section. Application of short-time Fourier transform (STFT) for point to point VSC-HVDC is presented in [8], using only 2-level VSC topology. The transients due to sudden load changes are also investigated in the proposed method. However, the algorithm is only proposed for point-to-point HVDC and is not tested for VSC-MTDC grids. It also did not use the distributed frequency-based models of cables in the model.

Wavelet transform (WT), DFT and STFT are the main signal processing methods used to design power system protection algorithms. Both WT and STFT have advantages and drawbacks in fault signal processing, particularly in frequency domain analysis. Considering a particular window size, STFT gives more accurate frequency information than WT, while the multi-resolution analysis in WT results in a trade-off between time and frequency information. This paper investigates the application of STFT for fault analysis of VSC–MTDC systems, concentrating on DC section and different DC fault types. The frequency spectrum of fault transients is used for protection study, which works similar to a definite-time overcurrent method. Other than detecting the faulty section, an index is defined for faulty pole detection. A modified version of CIGRE DCS2 MTDC test system introduced in [9] is simulated in PSCAD and the signal processing is handled by spectrogram function in MATLAB. In order to have more detailed study, sensitivity analysis of the important STFT parameters like window size and hop size are presented. The remainder of this paper is organised as follows: Section 2 explains the protection method and gives a brief introduction of STFT. Section 3 describes the test system, and Section 4 discusses the simulation results. The sensitivity analysis is presented in Section 5, and finally Section 6 concludes the paper.

2 Proposed method

The proposed method utilises STFT as the main signal-processing tool for defining the protection method. Unlike other proposed methods, which use discrete frequency orders for fault detection and analysis, this research uses the frequency spectrum of discrete frequencies and inter-harmonics for protection analysis. The protection method works as a definite-time overcurrent algorithm, with two settings of normalised power/frequency value of spectrum and time duration. The frequency range used from the spectrum has an important role in fault detection accuracy. Fig. 1 shows a sample processed fault transient. Looking at the frequency spectrum in the figure, the frequency spectrum range between 2 and 4 kHz is chosen for the protection method in all tests. This range suits the detection of faults with different locations and resistances in the proposed system.
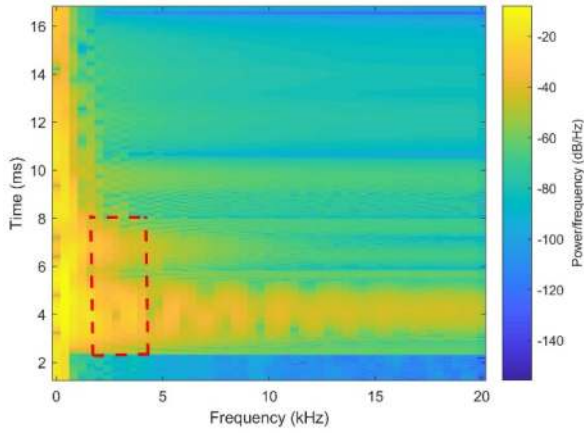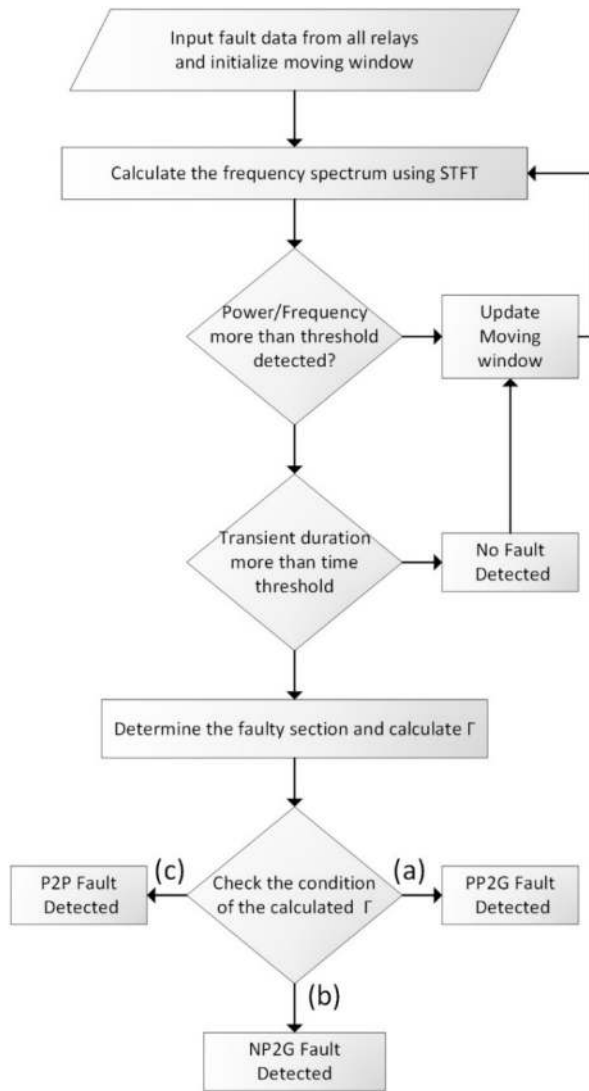
Fig. 1 *Frequency spectrum of a sample transient*

Fig. 2 *Flowchart of the proposed method*

2.1 Short-time Fourier transform

The main difference between STFT and Fourier transform (FT) is that in STFT the signal is divided into multiple sections, where each of them is considered stationary. A window function ($\omega(t)$) with the size equal to each section is chosen from the available window types like Rectangular, Hanning, Bartlett etc. and is placed in the beginning of the signal. Based on the Hop size, the window will shift along the signal, repeating the Fourier transform for the new window with updated wave data. In fact, based on the sampling frequency and the Hop size, a number of samples will be released from the end of the windows and the same number will be added in the front, making a time-based move. The following equations represent the continuous and discrete versions of STFT, respectively:

$$\text{STFT}(t\omega) = \int_{-\infty}^{+\infty} [x(t)\omega(t - t')]e^{-j2\pi ft}dt \quad (1)$$

$$\text{DSTFT}(mk) = \sum_{n=0}^{n=N-1} [x(n)\omega(n - mH)]e^{-j(2\pi nk/(N))} \quad (2)$$

where N is the number of FFT points, $x(n)$ is the input function, $\omega(n)$ is the window function, n is the umber of input samples and H is the hop size. Actually, STFT is the FT of the signal multiplied by a window function in complex conjugate form. The time resolution highly depends on the hop size, resulted from the below equation

$$k = \frac{N_x - N_{\text{overlap}}}{N_\omega - N_{\text{overlap}}} \quad (3)$$

where k is the amount of data in time axis, N_x is the data length, N_ω is the window length and N_{overlap} is the window size minus the hop size. The higher the k, the better the time resolution.

2.2 Faulty pole detection

Based on multiple tests and observations in different fault simulations, fault transients have almost the same absolute maximum magnitude for both poles on the pole-to-pole faults, while having opposing polarity values. In positive or negative pole-to-ground faults, the magnitudes for positive and negative polarities are different, meaning the faulty pole has bigger transient magnitude. Thereupon, an index based on the maximum power/ frequency detected in STFT spectrum is defined in order to recognise the type of fault and faulty pole as given below

$$\Gamma = \left| \frac{P/f_{\text{pp}}}{P/f_{\text{np}}} \right| \quad (4)$$

where P/f_{pp} and P/f_{np} are the maximum value detected in power/ frequency spectrum for positive and negative to the ground faults, respectively. If this value be equal or close to unity, there is a pole-to-pole fault, for values bigger than unity and below it, there will be a positive pole and negative pole to the ground fault, respectively. An error value of 0.05 is considered for unity value, resulting the conditional equation for fault type detection

$$\begin{cases} 0 < \Gamma < 0.95 \text{ range } a \\ 0.95 < \Gamma < 1.05 \text{ range } b \\ 1.05 < \Gamma \text{ range } c \end{cases} \quad (5)$$

This method is true for the relays of the two sides of the faulty section, while for relays on the other faulty sections, the proposed rule may not be established. Therefore, it is necessary to do the detection of fault type and faulty pole step after discriminating the faulty section.

2.3 Protection algorithm

Based on the descriptions in this section, the flowchart of the proposed protection algorithm is depicted in Fig. 2.

3 Test system

A modified version of CIGRE B4 DCS2 system is simulated in PSCAD/EMTDC for fault transient analysis. The default radial topology is changed to a meshed grid, by adding a cable branch between Cm-B2 and Cm-E1. The single line diagram of the test system is shown in Fig. 3 and the system data is given in [9]. The converters are half-bridge modular multi-level converters with nearest level control switching method. Simulation and system

Fig. 3 *Single line diagram of modified CIGRE MTDC model*

Table 1 Main setting used for the protection algorithm

Relay time setting	Relay power/frequency setting	Sampling frequency	Window size	Hop size
3 ms	−30 dB/Hz	40 KHz	100 samples	1 sample

Table 2 Fault configurations for the Case studies

Fault no.	Fault type	Duration, ms	Location
i	P2P	1	zone B
II	PP2G	5	zone B

Table 3 Simulation results for Case I

Relay no.	Detected fault duration, ms	Max. power/frequency, dB/Hz		Relay operated	Faulty pole
		P. pole	N. pole		
8	no detection	—	—	×	—
3	<2	−33	−34	×	—
4	<1	−36.5	−35	×	—
6	no detection	—	—	×	—

Fig. 4 *Fault current harmonic spectrum of the positive pole relays for Case I using STFT. a = r.8, b = r.3, c = r.4 and d = r.6*

parameters are given in Table 1. Although 3 ms is long for a fault in VSC, this value is set for demonstration purposes. The Hop size is set to 1 sample, which is discussed in Section 5. The fault wave diagrams are exported to MATLAB and STFT is handled by '*Spectrogram*' function and signal processing toolbox. For page limitations, only the diagrams of relays 3, 4, 6 and 8 have been chosen in the case studies.

4 Simulation results

Two different fault configurations are applied to the test system. Table 2 shows the configurations of the faults. The first fault is a small pole-to-pole transient with small duration, while the next fault is longer. The second fault is a positive pole to the ground applied to the same zone. Both faults are applied to the same position, in zone B, which is an underground cable. Zones B and C are counted together as one transmission section, seen by relays 4 and 3, as a combination of overhead line (OHL) and underground cable.

4.1 Case I

In the first case, a short duration pole-to-pole fault transient is applied to zone B, which is an underground cable. Although most P2P faults in cables are permanent, the duration of 1 ms is considered for this transient as a test case. Based on the time-threshold setting of the relays and the system fault ride through capability, the system withstands through the fault and stays in normal operation without tripping. Table 3 and Figs. 4*a–d* show the results and fault wave diagrams for relays 8, 3, 4 ad 6, respectively.

4.2 Case II

In the second case, a positive pole to ground fault is applied on zone B with the duration of 5 ms. Table 4, Figs. 5 and 6 show the simulation results, fault waves and processed STFT spectrum for relays 8, 3, 4 and 6, respectively.

Based on the duration of maximum power/frequency detected on the spectrums shown in Fig. 6 and the relay settings, relays 3 and 4 will operate, while the other relays will not detect the fault.

Table 4 Simulation results for Case II

Relay no.	Detected fault duration, ms	Max. power/frequency, dB/Hz		Relay operated	Faulty pole
		P. pole	N. pole		
8	<2.5	—	—	×	—
3	~5	−24	−41	√	P. pole
4	~4.5	−25	−35	√	P. pole
6	<2	—	—	×	—
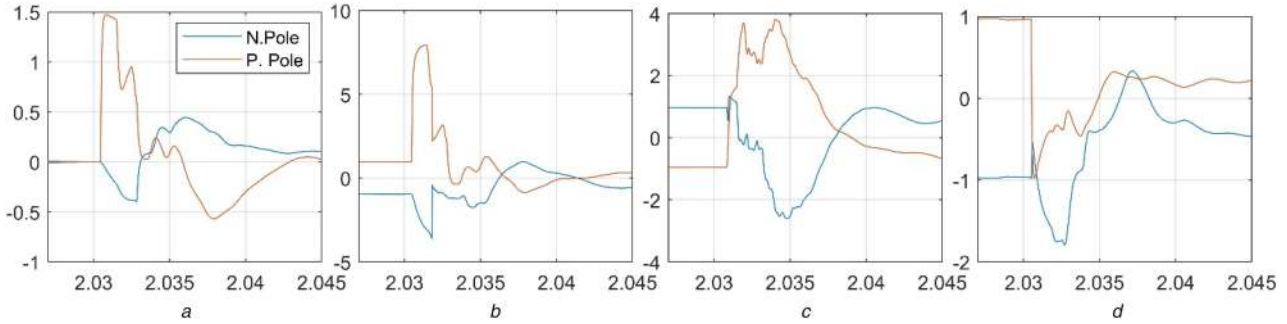
Fig. 5 *Fault current waves of the positive and negative pole for Case II using STFT. a = r.8, b = r.3, c = r.4 and d = r.6*
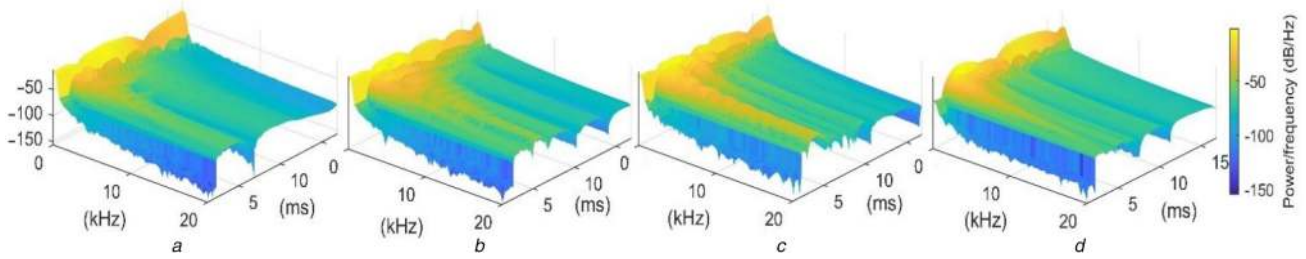
Fig. 6 *Fault current harmonic spectrum of the positive pole for Case II using STFT. a = r.8, b = r.3, c = r.4 and d = r.6*
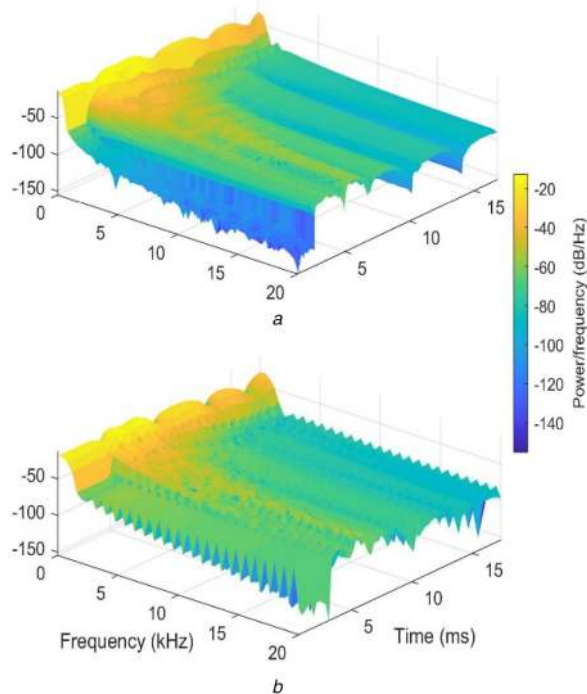
Fig. 7 *STFT-based spectrum of relay 3 in Case II with different window sizes*
(a) 100 samples, *(b)* 50 samples

The next step is the detection of the faulty pole. Calculation of Γ from (4), results values of 0.58 and 0.71 for relays 3 and 4, respectively, which are in range (b) according to (5), meaning a positive pole to the ground is detected. The latter can also be resulted from Fig. 5, which shows the difference in the waveform when different fault types happen in the system.

5 STFT parameters sensitivity analysis

STFT is very sensitive to the window size and hops size. Any change in STFT parameters results in significant changes in fault detection accuracy. The following section investigates the impact of STFT parameters in fault detection. The spectrum of a sample relay with different window sizes of 100 and 50 samples and the spectrum of a sample transient with different hop sizes of 1 and 15 samples for the moving window are investigated.

5.1 Impact of the window size

The window size is the most important factor in STFT, which defines the frequency resolution. The bigger the windows size, the better frequency resolution, but resulting less accurate time resolution. Fig. 7 compares the frequency resolution of relay 3 in Case II for two different window sizes of 100 and 50 samples, respectively. It is clear from Fig. 7 that the 50-sample window does not give accurate representation of frequencies, leading to a saw-tooth wave spectrum. If the windows size is too big, the time resolution will have unacceptable accuracy. Based on the sampling frequency, required time resolution and the application type, a 100 sample window size is chosen for this study.

5.2 Impact of the Hop size

The hop size has the most impact on the time resolution in STFT. The time resolution plays the main role in fault detection, which must be detected in the first milliseconds of occurrence. Fig. 8 shows the STFT diagram of relay 6 in Case II for two different hop sizes of 1 and 10 samples, respectively. It is obvious that the fault detection is more accurate with the hope size of one sample because of better time resolution especially in the first 5 ms of fault occurrence. Actually, the time axis spectrum became smoother in
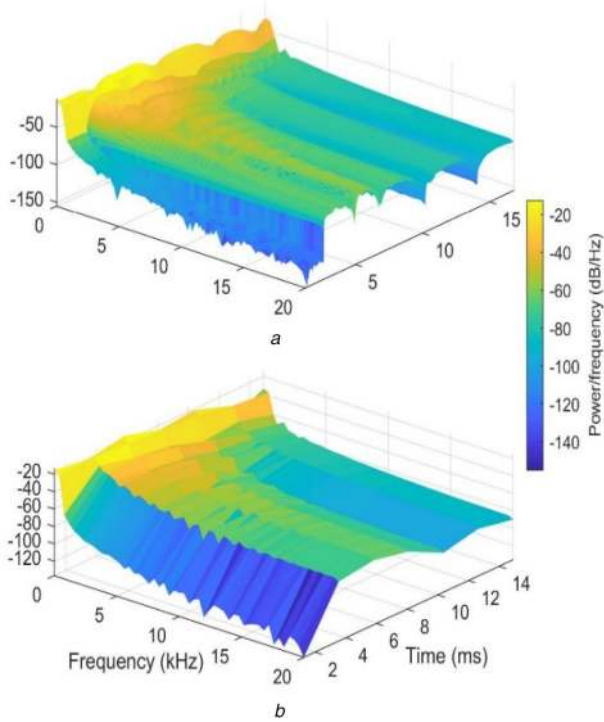
Fig. 8 *STFT-based spectrum of a sample transient with different hop sizes*
(a) 1 sample, *(b)* 15: samples

the diagram with 15 sample hop size, meaning less accurate time resolution because of having lower amount of data, based on (3).

5.3 Impact of the window type

There are a number of window types for use in STFT. The most common types are Rectangular, Hanning, Triangular, Hamming, and Bartlett. After multiple tests, there were no significant difference in results between the window types and finally the rectangular window had been chosen for all cases.

6 Conclusion

Application of STFT for harmonic-based protection of meshed VSC-MTDC grids is studied in this paper. The proposed protection algorithm works in the same topology as a definite-time overcurrent relay with time and normalised power/frequency setting values. When relays detect transient data with the values bigger than the relay's setting values, the faulty section is determined. Afterwards, the faulty pole is determined with the calculation of a predefined index Γ. The sensitivity analysis shows the importance of window and hop size for STFT, which have a significant impact on the accuracy of the proposed protection method. Further research will consist of determining the accurate fault location in OHLs and underground cables in VSC-MTDC grids using STFT and harmonic based algorithms.

7 References

[1] Farhadi, M., Mohammed, O.A.: 'Protection of multi-terminal and distributed DC systems: design challenges and techniques', *Electr. Power Syst. Res.*, 2017, **143**, (Supplement C), pp. 715–727
[2] Tzelepis, D., Dyśko, A., Fusiek, G.*, et al.*: 'Single-ended differential protection in MTDC networks using optical sensors', *IEEE Trans. Power Deliv.*, 2017, **32**, (3), pp. 1605–1615
[3] Zhang, X., Tai, N., Wang, Y.*, et al.*: 'EMTR-based fault location for DC line in VSC–MTDC system using high-frequency currents', *Transm. Distrib. IET Gener.*, 2017, **11**, (10), pp. 2499–2507
[4] Liu, J., Tai, N., Fan, C.: 'Transient-voltage-based protection scheme for DC line faults in the multiterminal VSC-HVDC system', *IEEE Trans. Power Deliv.*, 2017, **32**, (3), pp. 1483–1494
[5] Yang, Q., Le Blond, S., Aggarwal, R.*, et al.*: 'New ANN method for multi-terminal HVDC protection relaying', *Electr. Power Syst. Res.*, 2017, **148**, (Supplement C), pp. 192–201
[6] Zheng, Z., Tai, T., Thorp, J.S.*, et al.*: 'A transient harmonic current protection scheme for HVDC transmission line', *IEEE Trans. Power Deliv.*, 2012, **27**, (4), pp. 2278–2285
[7] Zheng, X., Tai, N., Wu, Z.*, et al.*: 'Harmonic current protection scheme for voltage source converter-based high-voltage direct current transmission system', *Transm. Distrib. IET Gener.*, 2014, **8**, (9), pp. 1509–1515
[8] Satpathi, K., Yeap, Y.M., Ukil, A.*, et al.*: 'Short-time Fourier transform based transient analysis of VSC interfaced point-to-point DC system', *IEEE Trans. Ind. Electron.*, 2017, **PP**, (99), pp. 1–1
[9] 'The CIGRE B4 DC grid test system'. Available at https://e-cigre.org/publication/ELT_270_9-the-cigre-b4-dc-grid-test-system, accessed January 2018